5th International Conference on Durability of Concrete Structures
Jun 30–Jul 1, 2016
Shenzhen University, Shenzhen, Guangdong Province, P.R.China

Aggregate Shape Effect on Multicomponent Ionic Electromigration in Concrete

Qing-feng Liu and Jian Yang
State Key Laboratory of Ocean Engineering, Shanghai Jiao Tong University, Shanghai 200240, P.R.China

Long-yuan Li
School of Marine Science and Engineering, University of Plymouth, PL4 8AA, UK

Jian Yang
School of Civil Engineering, University of Birmingham, B15 2TT, UK

ABSTRACT

This paper presents a numerical study on the mechanism of chloride migration in concrete. Unlike most of existing work, this study utilises multicomponent ionic transport models to reflect the influence of ionic interactions by coupling both mass conservation and Poisson's equations. A series of 2-D, 3-phase models with different shapes and volume fractions of aggregates are developed to simulate the chloride migration test. Through a comparatively overall numerical exploration that considers external voltage, ionic interactions, heterogeneous nature, ITZ, and ionic binding, some important features about multispecies coupling and aggregate shape effect, which have not been properly reported from existing concrete models, are highlighted.

1. INTRODUCTION

Nowadays, chloride-induced corrosion of reinforced concrete (RC) structures has becoming a worldwide problem. It affects a large number of public infrastructure and buildings, particularly those used in offshore or exposed in marine environment. In order to prevent reinforcing bar from corrosion, one has to know the mechanism about how chlorides penetrate in concrete and how individual components in concrete respond while chlorides enter the concrete.

To characterise the transport behaviour of ionic species in concrete, during the last decades, great efforts have been made on the assessment of ionic transport by using traditional approaches, i.e., analytical models (Atkinson & Nickerson, 1984; Byung & Seung, 2004) and/or experimental techniques (AASHTO T 259, 2003; ASTM C1543, 2010; NT Build 443, 1995; ASTM C1556, 2011; Whiting, 1981; AASHTO T 277, 1983; ASTM C 1202, 1994; Tang & Nilsson, 1993a; NT-Build 492, 1999; AASHTO TP 64-03, 2003). However, note that concrete is a heterogeneous material with complicated meso- and microstructure organisations, e.g., coarse/fine aggregate, cement paste, capillary/gel pores, and cracks. For analytical studies, the main shortcoming is that they could only focus on the transport of ions in a 1-D single-phase medium (i.e., the cement or mortar matrix), neglecting the impact of inner structures of concrete. Moreover, due to the high non-linear level of the problem of multicomponent ionic transport, almost all existing analytical models consider the transport of only a single species, i.e., the chloride ions. For experimental studies, though they can provide wider and valuable data, it is still very difficult for them to reveal individual effects of different factors because of the interactions between different factors. Also, most of testing methods are expensive and time consuming, especially for the high-performance concrete specimens.

As neither of the abovementioned method is appropriate to tackle the influences of individual components on chloride transport in concrete, finite element numerical models, originally developed for the stress analysis of concrete, have recently been applied to investigate the transport properties of concrete with multiple phases (Bentz & Garboczi, 1991; Bourdette, Ringot, & Ollivier, 1995; Caré, 2003; Caré & Hervé, 2004; Garboczi & Bentz, 1998; Jiang, Sun, & Wang, 2013; Li, Xia, & Lin, 2012; Sun, Zhang, Sun, Liu, & Wang, 2011; Xiao, Ying, & Shen, 2012; Yang & Weng, 2013; Ying, Xiao, Shen, & Bradford, 2013; Zeng, 2007; Zheng, Wong, & Buenfeld, 2009). By using this type of multiphase computational model, one can easily clarify and quantify the influence cause by different structure of concrete, i.e., inclusion aggregates, mortar/cement, and interfacial transition zones (ITZs), which cannot be fulfilled in 1-D analytical models. However, most of above work assumed circular or spherical particles for aggregates during modelling and this gross simplification may cause inaccuracy in simulation results. More recently, researchers further established mesostructures of concrete with several aggregate shapes to explore the aggregate shape

effect on chloride diffusion in concrete. For example, Zheng, Zhou, Wu, and Jin (2012) developed a 2-D, 3-phase lattice model to investigate the shape effect of elliptical aggregate on chloride diffusion in concrete. They concluded that when the chloride diffusivity in concrete decreases with the increase of aspect ratio of elliptical aggregate particles. Abyaneh, Wong, and Buenfeld (2013) presented a 3-phase FEA model in 3-dimension to investigate the shape effect of various spheroidal aggregates (i.e., spherical, tri-axial ellipsoidal, prolate spheroidal, and oblate spheroidal) and found that the diffusivity significantly decreased when spherical aggregate particles were replaced by ellipsoidal aggregate particles, particularly for higher aggregate fractions and aspect ratios.

Above numerical studies considered a diffusion problem and employed the Fick's first law to govern the steady-state chloride penetration in cracked concrete. In view of the long duration of diffusion tests and the need of electrochemical rehabilitation, the action of externally applied electric field is prevalently involved in a bunch of numerical models of chloride transport in concrete (Feng, Li, Kim, & Liu, 2016; Frizon, Lorente, Ollivier, & Thouvenot, 2003; Jensen, Johannesson, & Geiker, 2014; Johannesson, Yamada, Nilsson, & Hosokawa, 2007; Krabbenhoft & Krabbenhoft, 2008; Li, Easterbrook, Xia, & Jin, 2015; Li & Page, 1998; Liu, Easterbrook, Yang, & Li, 2015; Liu, Li, Easterbrook, & Yang, 2012; Liu & Shi, 2012; Liu, Xia, Easterbrook, Yang, & Li, 2014; Liu et al., 2015; Narsillo, Li, Pivonka, & Smith, 2007; Samson & Marchand, 2007; Toumi, Francois, & Alvarado, 2007; Truc, Ollivier, & Nilsson, 2000; Wang, Li, & Page, 2001; Xia & Li, 2013; Šavija, Luković, & Schlangen, 2014). These models extended the ionic diffusion to a more complicated migration dominated process, which follows the applications of the rapid chloride permeability/migration (RCP/RCM) test (Whiting, 1981; AASHTO T 277, 1983; ASTM C 1202, 1994; Tang & Nilsson, 1993a; NT-Build 492, 1999; AASHTO TP 64-03, 2003) and the electrochemical chloride removal/extraction (ECR/ECE) treatment (Lankard, Slatter, Holden, & Niest, 1975). However, the convection-dominated diffusion equations caused due to the presence of external electric field can create some numerical difficulties both in meshing and computing due to the Peclet number issue (Liu et al., 2012; Xia & Li, 2013; Šavija et al., 2014). Thus, in order to achieve convergent results, all of these studies only adopted the models of 1-D without aggregate phase or 2-D but only with circular aggregates for simplification.

The literature survey described above shows that the aggregate shape effect on the transport properties of mortar or concrete has not been investigated in existing numerical models, which take the action of externally applied electric field into account. In this paper, a numerical study is presented for theoretically investigating the aggregate shape effect during multiple ionic electromigration process within concrete. A series of 2-D, 3-phase models with different shapes and volume fractions of aggregates are developed to simulate the chloride migration (RCM) test. Note that existing studies on aggregate shape effect (Abyaneh et al., 2013; Zheng et al., 2012) did not discuss or show the details of chloride transport in concrete, e.g., the time-dependent penetration depth (which is the key information for calculating diffusivity *via* RCM test) and only modelling concrete with spheroidal-shaped inclusions (which may decrease the tortuosity of ionic transport path to some extent). The presented study examines both spheroidal and polygon aggregates and also provides time and spatial distribution results of four involved ionic species (K^+, Na^+, Cl^-, OH^-) by solving both mass conservation and Poisson's equations. Through a comparatively overall numerical exploration, including external voltage, ionic interactions, binding effect, ITZs, non-steady-state process, and aggregate shape factor, some important features, which have not been properly reported from existing concrete transport models, are highlighted.

2. THEORETICAL BACKGROUND

Concrete pore solution is a multicomponent electrolyte involving not only chloride ions but also other ions, such as sodium, potassium, hydroxyl, sulphate, and calcium. For the cases of diffusion tests, the transport of ions in a saturated concrete is mainly driven by the concentration gradient of the species itself and can be described as Fick's first law, which is most utilised in the durability study of the cracked concrete (Abyaneh et al., 2013; Bentz & Garboczi, 1991; Bourdette et al., 1995; Caré, 2003; Caré & Hervé, 2004; Garboczi & Bentz, 1998; Jiang et al., 2013; Li et al., 2012; Sun et al., 2011; Xiao et al., 2012; Yang & Weng, 2013; Ying et al., 2013; Zeng, 2007; Zheng et al., 2009, 2012). When the electrostatic potential is involved such as in migration tests (Whiting, 1981; AASHTO T 277, 1983; ASTM C 1202, 1994; Tang & Nilsson, 1993a; NT-Build 492, 1999; AASHTO TP 64-03, 2003), the more significant driving force of ionic transport is the electrostatic potential gradient, in which case the flux of an ionic species can be expressed using the Nernst–Planck equation as follows:

$$\mathbf{J}_k = -D_k \nabla C_k - D_k C_k \frac{z_k F}{RT} \nabla \Phi \tag{1}$$

where $\boldsymbol{J}_k$ is the flux, C_k is the concentration, D_k is the diffusion coefficient (note that in the heterogeneous concrete model, D_k has to be defined separately in different phases), z_k is the charge number, $F = 9.648 \times 10^{-4}$ Cmol^{-1} is the Faraday constant, $R = 8.314$ J mol^{-1}K^{-1} is the ideal gas constant, $T = 298$ K is the absolute temperature, Φ is the electrostatic potential, and the subscript k represents the k-th ionic species. Assume that the concrete is

saturated and there is no chemical reaction taking place between ionic species, the following mass conservation defined in unit volume of electrolyte solution for each individual ionic species can be obtained,

$$\frac{\partial C_k}{\partial t} = -\nabla \cdot \mathbf{J}_k \tag{2}$$

where t is the time. When applying the ionic transport equations from an electrolyte solution to a porous material, one has to consider the ionic binding at pore surface. Therefore, Eq. (2) need to be modified as follows:

$$\frac{\partial C_k}{\partial t} + \frac{\partial S_k}{\partial t} = -\nabla \cdot \mathbf{J}_k \tag{3}$$

where S_k is the concentration of bound ions of species k. It is suggested that the relationship between the bound and free chloride concentrations is almost independent of its transport rate and may satisfies the linear, Langmuir, or Freundlich isotherm (Tang & Nilsson, 1993b) depending on its concentration. Recent work by Bentz et al. (2013) highlighted the significant role of binding effect during the ingress of chlorides in cracked concrete, and it is suggested to utilise a simple linear isotherm to express the relationship between free and bound ions for enhancing numerical stability,

$$S_k = \lambda C_k \tag{4}$$

where λ a is a dimensionless fitting constant. Note that for constant λ, the term $(1 + \lambda)$ can be absorbed into the time term, and in this case the difference between the considerations of binding and non-binding does not affect the governing equation and is only reflected by a time factor. Substituting Eqs. (1) and (4) into Eq. (3), it yields,

$$(1+\lambda)\frac{\partial C_k}{\partial t} = \nabla(D_k \nabla C_k) + \nabla\left[\left(\frac{z_k D_k F}{RT}\right) C_k \nabla \Phi\right] \tag{5}$$

In most of numerical models considering multispecies transport in concrete (Frizon et al., 2003; Jensen et al., 2014; Li & Page, 1998; Liu & Shi, 2012; Liu et al., 2014; Narsillo et al., 2007; Toumi et al., 2007; Truc et al., 2000; Wang et al., 2001; Šavija et al., 2014), the electrostatic potential is often determined by using the assumption of electroneutrality condition. This implies that the spatial electrostatic potential is purely caused by the externally applied electric field and the charge balance of species occurs everywhere in the solution domain. In this case, the concentration of each ionic species can be calculated independently using Eq. (5) by employing $\nabla^2 \Phi = 0$. Apparently, this assumption makes the multispecies transport behave as a single-component model, which does not reflect the actual interaction between different ionic species (Liu et al., 2015). In order to accurately describe the internal charge imbalance between different species and also achieve the true multispecies coupling, recent work (Johannesson et al., 2007; Krabbenhoft & Krabbenhoft, 2008; Liu et al., 2012; Samson & Marchand, 2007; Xia & Li, 2013) suggested that one should use the following Poisson's equation to govern the electrostatic potential in the transport medium:

$$\nabla^2 \Phi = -\frac{F}{\varepsilon_0 \varepsilon_r} \sum_{k=1}^{N} z_k C_k \tag{6}$$

where $\varepsilon_o = 8.854 \times 10^{-12}$ CV^{-1} m^{-1} is the permittivity of a vacuum, $\varepsilon_r = 78.3$ is the relative permittivity of water at temperature of 298 K, and N is the total number of ionic species involved in the solution. For numerical modelling, the use of Poisson's equation creates two difficulties. One is the coupling of Eq. (5) between different ionic species, since Φ is now dependent on not only the boundary conditions defined by the externally applied electric field but also the concentrations of all ionic species involved in the medium. The other is the non-linearity and numerical difficulty, which involves calculations of large and small numbers that need be handled carefully (Liu et al., 2012; Xia & Li, 2013). Nevertheless, Eqs. (5) and (6) can be used to determine the electrostatic potential, Φ, and the concentrations of individual ionic species, C_k ($k = 1, 2, \ldots, N$), at any time and any point in the solution domain, provided that the initial and boundary conditions are properly defined.

3. MODELING

The concrete modelled in this study is treated as a heterogeneous composite structure with three phases consisting of mortar matrix, coarse aggregates, and ITZs. Most of the existing multiphase models (Bentz & Garboczi, 1991; Bourdette et al., 1995; Caré, 2003; Caré & Hervé, 2004; Garboczi & Bentz, 1998; Jiang et al., 2013; Sun et al., 2011; Xiao et al., 2012; Yang & Weng, 2013; Ying et al., 2013; Zeng, 2007; Zheng et al., 2009) including previous work as well (Feng et al., 2016; Liu, Easterbrook et al., 2015, Liu et al., 2015, 2012, 2014; Šavija et al., 2014), assumed circular or spherical aggregates for simplification. Figure 1 shows one of the 2-D concrete numerical models with the size of 50 mm $\times$ 50 mm. The volume fraction of aggregates is $V_{agg} = 0.5$. In the figure, all circular areas represent the impermeable aggregates with the radii ranging from 1.5 to 10 mm. Outside each aggregate, there is an aureole ITZ shell of tiny scale (40 μm) wrapping the aggregate. Outside the ITZs, the remaining part of the concrete model represents the mortar matrix. The location of the aggregates was randomly generated using a MATLAB program. It should be mentioned that, the shape of aggregates may not be perfectly

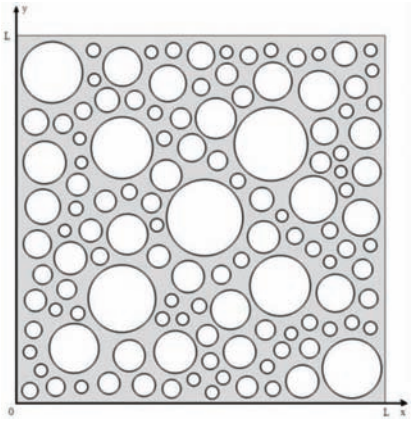

Figure 1. With figures centred in columns like this at different w/s ratio after 7, 14, and 28 days.

circular in reality. Thus, in order to further investigate the effect caused by aggregate shapes and volume fractions, a set of 2-D concrete numerical models with various shapes and volume fractions of coarse aggregates were developed herein.

Figure 2 shows the meshed models with the same aggregates volume fraction of $V_{agg} = 0.5$ but different aggregates shapes: ellipse, triangle, rectangle, and mixed shapes. As the aggregates are assumed to be impermeable, only the mortar phase is meshed. It is also noticeable from Figure 2 that, the distributions of ellipse, triangle, rectangle aggregates are almost uniform, whereas only that of mixed shaped aggregates is less uniform. A careful examination of the geometry including mixed particles shows that, the smaller sized particles gather more in the region near the cathode (from x = 0 to x = 0.025), whereas the larger ones gather more in the region near the anode (from x = 0.025 to x = 0.05). This setting is deliberately arranged for legible exploration of the influence of tortuosity, which will be explained later in discussions.

The model described above is used to simulate the RCM test of concrete, in which the 50 mm × 50 mm plain concrete specimen is located between two compartments, one of which has a 0.52-mole/l NaCl solution, the other of which has a 0.30-mole/l NaOH solution. An external potential difference of 24 V is applied between two electrodes inserted into the two compartment solutions. The ionic species to be analysed in the simulations include potassium, sodium, chloride, and hydroxyl. Note that other ionic species (such as calcium and sulphate) may also exist in the concrete. However, owing to their low concentrations they are not considered in the present simulations. The ionic transport parameters employed for different phases are listed in Table 1. Figure 3 graphically displays the simulated test. Note that since the volume of either compartment is much greater than that of the specimen, it is reasonable to assume that the concentrations of each ionic species in the two compartments remain constants during the migration test. Table 2 shows the initial and boundary conditions employed in the present study.

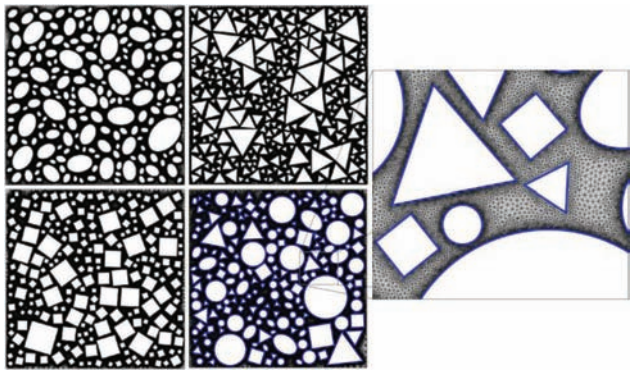

Figure 2. Finite element mesh of geometries with various shaped aggregates, $V_{agg} = 0.5$.

Table 1. Ionic transport properties in different phases.

Field variables	K^+	Na^+	Cl^-	OH^-
Charge number	1	1	–1	–1
Diffusion coefficient in aggregates, D_A	0	0	0	0
Diffusion coefficient in bulk mortar, $D_{B,} \times 10^{-10}$ m²/s	3.914	2.668	4.064	10.52
Diffusion coefficient in ITZs, D_I, $\times 10^{-9}$ m²/s	1.174	0.800	1.219	3.156

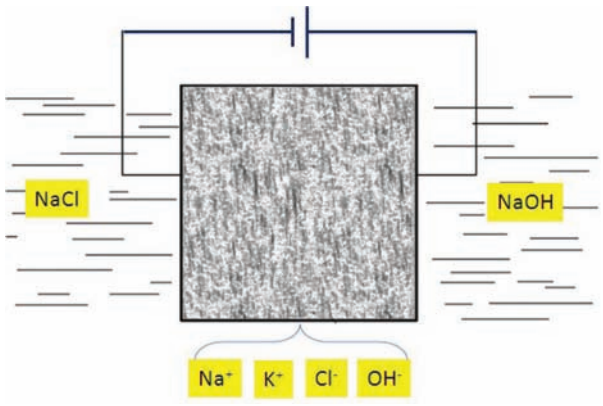

Figure 3. Schematic representation of 2-D plain concrete specimen in a RCM test.

Table 2. Initial and boundary conditions of individual species.

Field variables		K^+	Na^+	Cl^-	OH^-	Φ
C, mole/m³	x = 0	0	520	520	0	0
	x = L	0	300	0	300	24 V
Flux	y = 0	J = 0	J = 0	J = 0	J = 0	əΦ/əy = 0
	y = L	J = 0	J = 0	J = 0	J = 0	əΦ/əy = 0
Initial, mole/m³	t = 0	200	100	0	300	0

4. RESULTS AND DISCUSSION

For given initial and boundary conditions, the ionic transport in the simulated concrete specimens can be numerically calculated by solving the mass conservation equation and Poisson equation. As particular interest is of the penetration of chloride ions, here, only the chloride distribution profiles are displayed in the form of the 3-D plot, which are shown in Figures 4–8. Generally speaking, with the same aggregates volume fraction, the evolutions of ionic transports in the models filled by ellipse, triangle, rectangle, and mixed shaped aggregates closely resemble that in the circular-shaped model. The negatively charged chlorides steadily move from the cathode towards the anode by electromigration process, which takes place mainly along the x-axis direction. It also can be seen from the figures that, the aggregates split the migration wave fronts into a number of pieces which makes the wave front act like a "waterfall." Generally, the pieces of "waterfall" move at a synchronous velocity throughout the most 3-D figures. However, in the triangle-shaped aggregate model (Figure 6), it is noticeable that the speeds of the "waterfall" pieces are not parallel and ordered. This phenomenon can be explained by the effect of tortuosity. The sharp angle of triangle shape will markedly increasing the length of the flow paths as well as generates many local corner pockets in the electrolyte solution to decrease the transport of ions in corresponding areas.

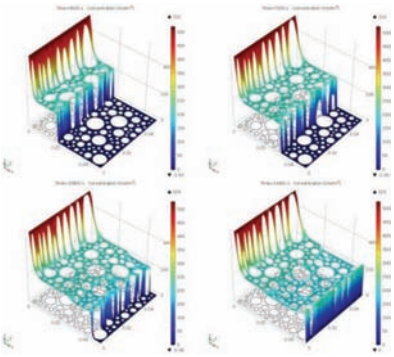

Figure 4. Concentration distribution profiles of chloride ions (for aggregates with a circular shape).

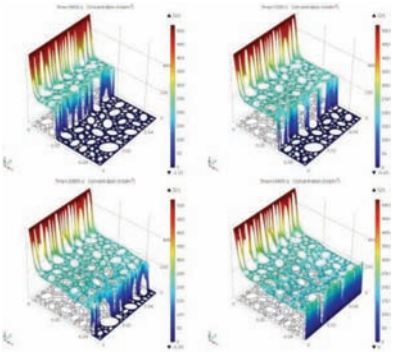

Figure 5. Concentration distribution profiles of chloride ions (for aggregates with an ellipse shape).

For a more quantitative study, Figures 9–12 give comparisons of concentration profiles of four ionic species between five different shapes when they have the same volume fraction of aggregates. It is clearly shown that, there is only a tiny difference in the migration velocities between the models with the shapes of circular, ellipse, and rectangle, which implies a similar tortuosity between the models with these shapes of inclusion. In contrast, from the overall points of view, the triangle-shaped aggregates bring a slower velocity than other shaped aggregates due to its largest tortuosity.

More interesting features are found in the mixed shaped aggregates. As it was mentioned above that

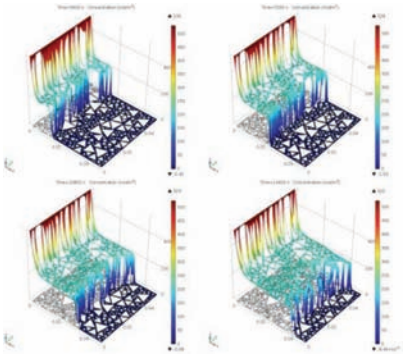

Figure 6. Concentration distribution profiles of chloride ions (for aggregates with a triangle shape).

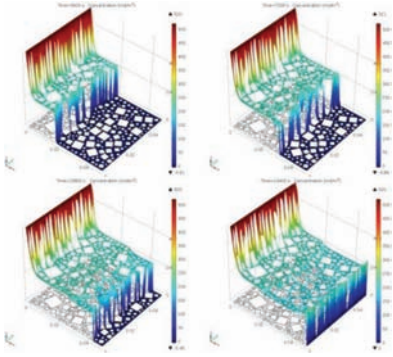

Figure 7. Concentration distribution profiles of chloride ions (for aggregates with a rectangle shape).

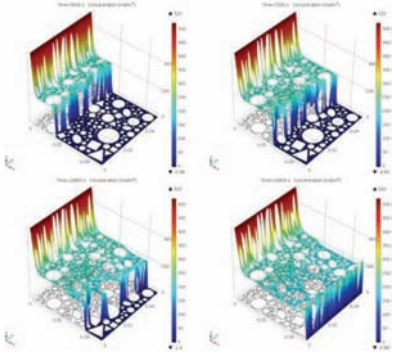

Figure 8. Concentration distribution profiles of chloride ions (for aggregates with mixed shapes).

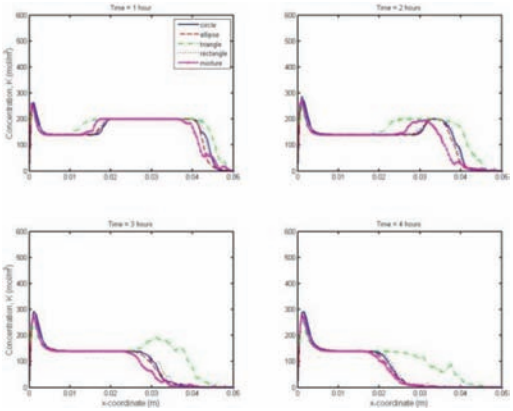

Figure 9. Comparisons of potassium concentration profiles between different aggregate shapes, $(1 - \phi) = 0.5$.

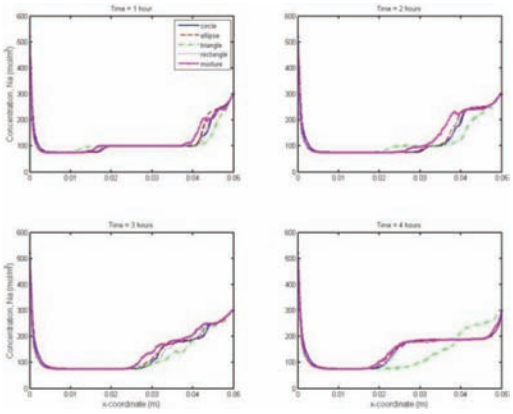

Figure 10. Comparisons of sodium concentration profiles between different aggregate shapes, $(1 - \phi) = 0.5$.

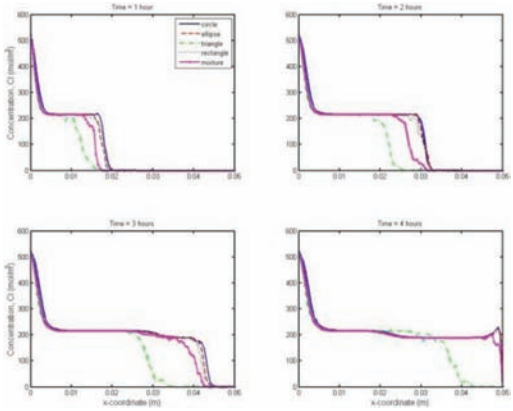

Figure 11. Comparisons of chloride concentration profiles between different aggregate shapes, $(1 - \phi) = 0.5$.

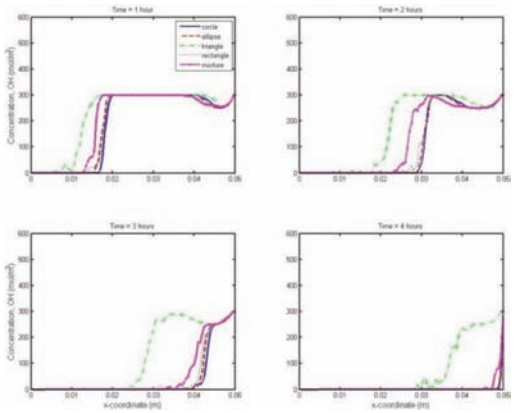

Figure 12. Comparisons of hydroxide concentration profiles between different aggregate shapes, $(1 - \phi) = 0.5$.

the distribution of the different sized aggregates are deliberately arranged to be less uniform (the smaller ones more gathers in the left side of the concrete specimen and the larger ones do the opposite), the tortuosity of the model including mixed shaped aggregates is correspondingly less uniform (larger tortuosity in region near the cathode and smaller tortuosity in region near the anode). As a consequence, when the migration waves of the negatively charged ions (both chloride and hydroxide) of the mixed shaped aggregates travel from the section of x = 0 to the section of x = 0.025, its speed is slower than the others, even including the triangle ones, when they travel from the section of x = 0.025 to the section of x = 0.05, the migration waves of the mixed shaped aggregates speed up, overtaking the triangle one and finally almost equalling the evolution of other three shaped aggregates at the region near the anode. This procedure exactly reverses when it happens to the positively charged ions (both potassium and sodium). The phenomenon described above evidently depicts how the tortuosity caused by the aggregate phase affects the ionic transport in concrete.

The above findings seem to indicate that, under the condition of identical volume fraction and similar tortuosity, the shape of aggregate has little impact on the penetrations of ions. To further prove this opinion, more examples are provided here of different shapes with different volume fractions. Figures 13 and 14, respectively, show the comparisons of different shapes under the aggregate volume fractions of $V_{agg} = 0.4$ and 0.3. As it was expected, both figures again show that the migration velocities of chlorides are approximately a constant between various shapes, except for the triangle aggregates, which has significantly larger tortuosity. Note that the aggregates of mixed shapes in this example are randomly distributed. Therefore, the special behaviour which occurs in Figures 9–12 disappears in Figures 13 and 14, in terms of the special results of triangle-shaped aggregates. Note that triangle-shaped aggregates are the extreme case which is very rare in reality. Therefore, it can be concluded that the influence of particle shapes on the permeability of concrete is not very significant.

In order to examine the influence of the volume fraction of aggregates on the ionic transport, particularly that of chloride ions, Figure 15 shows the concentration distribution profiles of chloride ions at four different times for three different aggregate volume fractions. It can be seen from the figure that, the influence caused by various volume fractions is much more remarkable

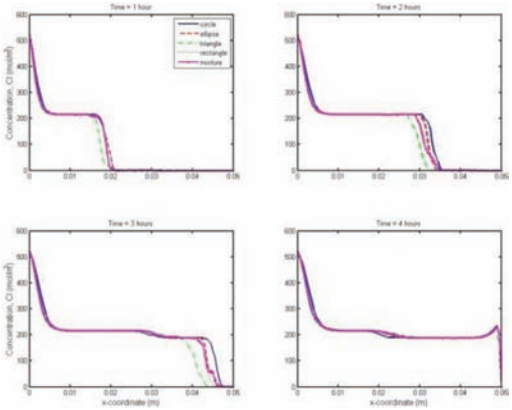

Figure 13. Comparisons of chloride concentration profiles between different aggregate shapes, $(1 - \phi) = 0.4$.

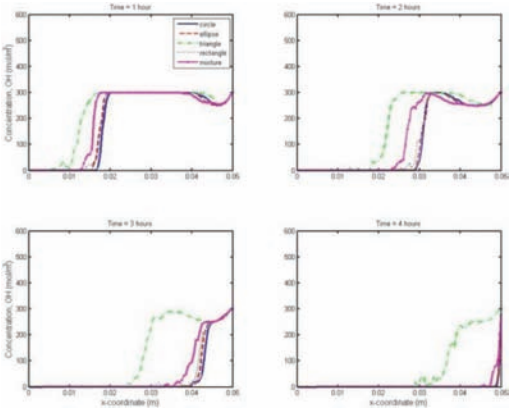

Figure 14. Comparisons of chloride concentration profiles between different aggregate shapes, $(1 - \phi) = 0.3$.

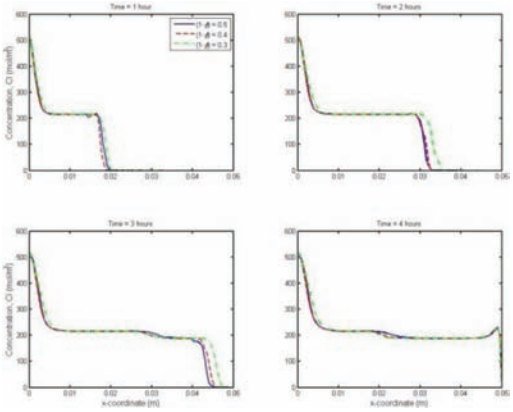

Figure 15. Comparisons of chloride concentration profiles between different volume fractions (circular aggregates).

than that caused by various shapes. Specifically, the smaller the aggregate volume fraction, the quicker the chloride ions can travel. The reason for this is still likely due to the effect of tortuosity, as the higher the aggregate volume fraction, the larger the tortuosity; therefore, the slower the ionic transport.

REFERENCES

AASHTO T 259. (2003). *Standard method of test for resistance of concrete to chloride ion penetration*. Washington, DC: American Association of States Highway and Transportation Officials.

AASHTO T 277. (1983). *Standard method of test for rapid determination of the chloride permeability of concrete*. Washington, DC: American Association of States Highway and Transportation Officials.

AASHTO TP 64-03. (2003). *Standard method of test for prediction of chloride penetration in hydraulic cement concrete by the rapid migration procedure*. Washington, DC: American Association of State Highway and Transportation Officials.

Abyaneh, S. D., Wong, H. S., & Buenfeld, N. R. (2013). Modelling the diffusivity of mortar and concrete using a three-dimensional mesostructure with several aggregate shapes. *Computational Materials Science, 78*, 63–73.

ASTM C 1202. (1994). *Standard test method for electrical indication of concrete's ability to resist chloride ion penetration*. Philadelphia, PA: American Society for Testing and Materials.

ASTM C1543. (2010). *Standard test method for determining the penetration of chloride ion into concrete by ponding*. West Conshohocken, PA: ASTM International.

ASTM C1556. (2011). *Standard test method for determining the apparent chloride diffusion coefficient of cementitious mixtures by bulk diffusion*. West Conshohocken, PA: ASTM International.

Atkinson, A., & Nickerson, A. K. (1984). The diffusion of ions through water-saturated cement. *Journal of Materials Science, 19*, 3068–3078.

Bentz, D. P., & Garboczi, E. J. (1991). Percolation of phases in a three-dimensional cement paste microstructural model. *Cement and Concrete Research, 21*(2–3), 325–344.

Bentz, D. P., Garboczi, E. J., Lu, Y., Martys, N., Sakulich, A. R., & Weiss, W. J. (2013). Modeling of the influence of transverse cracking on chloride penetration into concrete. *Cement and Concrete Composites, 38*, 65–74.

Bourdette, B., Ringot, E., & Ollivier, J. P. (1995). Modeling of the transition zone porosity. *Cement and Concrete Research, 25*(4), 741–751.

Brakel, J. V., & Heertjes, P. M. (1974). Analysis of diffusion in macroporous media in terms of porosity, a tortuosity and a constrictivity factor. *International Journal of Heat Mass Transfer, 17*(9), 1093–1103.

Byung, H. O., & Seung, Y. J. (2004). Prediction of diffusivity of concrete based on simple analytical equations. *Cement and Concrete Research, 34*(3), 463–480.

Caré, S. (2003). Influence of aggregates on chloride diffusion coefficient into mortar. *Cement and Concrete Research, 33*(7), 1021–1028.

Caré, S., & Hervé, E. (2004). Application of a n-phase model to the diffusion coefficient of chloride in mortar. *Transport Porous Media, 56*(2), 119–135.

Feng, G. L., Li, L. Y., Kim, B., & Liu, Q. F. (2016). Multiphase modelling of ionic transport in cementitious materials with surface charges. *Computational Materials Science, 111*, 339–349.

Frizon, F., Lorente, S., Ollivier, J. P., & Thouvenot, P. (2003). Transport model for the nuclear decontamination of cementitious materials. *Computational Materials Science, 27*, 507–516.

Garboczi, E. J. (1990). Permeability, diffusivity, and microstructural parameters: A critical review. *Cement Concrete Res, 20*(4), 591–601.

Garboczi, E. J., & Bentz, D. P. (1997). Analytical formulas for interfacial transition zone properties. *Advanced Cement Based Materials, 6*(3–4), 99–108.

Garboczi, E. J., & Bentz, D. P. (1998). Multiscale analytical/numerical theory of the diffusivity of concrete. *Advanced Cement Based Materials, 8*(2), 77–88.

Hobbs, D. W. (1999). Aggregate influence on chloride ion diffusion into concrete. *Cement and Concrete Research, 29*, 1995–1998.

Jensen, M. M., Johannesson, B., & Geiker, M. R. (2014). Framework for reactive mass transport: Phase change modeling of concrete by a coupled mass transport and chemical equilibrium model. *Computational Materials Science, 92*, 213–223.

Jiang, J. Y., Sun, G. W., & Wang, C. H. (2013). Numerical calculation on the porosity distribution and diffusion coefficient of interfacial transition zone in cement-based composite materials. *Construction and Building Materials, 39*, 134–138.

Johannesson, B., Yamada, K., Nilsson, L. O., & Hosokawa, Y. (2007). Multi-species ionic diffusion in concrete with account to interaction between ions in the pore solution and the cement hydrates. *Materials and Structures, 40*, 651–665.

Krabbenhoft, K., & Krabbenhoft, J. (2008). Application of the Poisson-Nernst-Planck equations to the migration test. *Cement and Concrete Research, 38*, 77–88.

Lankard, D. R., Slatter, J. E., Holden, W. A., & Niest, D. E. (1975). *Neutralization of chloride in concrete* (FHWA Report No. FHWA-RD-76-6). Battelle Columbus Laboratories.

Li, L. Y., & Page, C. L. (1998). Modelling and simulation of chloride extraction from concrete by using electrochemical method. *Computational Materials Science, 9*, 303–308.

Li, L. Y., Easterbrook, D., Xia, J., & Jin, W. L. (2015). Numerical simulation of chloride penetration in concrete in rapid chloride migration tests. *Cement and Concrete Composites, 63*, 113–121.

Li, L. Y., Xia, J., & Lin, S. S. (2012). A multi-phase model for predicting the effective diffusion coefficient of chlorides in concrete. *Construction and Building Materials, 26*(1), 295–301.

Liu, Q. F., Easterbrook, D., Yang, J., & Li, L. Y. (2015). A three-phase, multi-component ionic transport model for simulation of chloride penetration in concrete. *Engineering Structures, 86*, 122–133.

Liu, Q. F., Li, L. Y., Easterbrook, D., & Yang, J. (2012). Multi-phase modelling of ionic transport in concrete when subjected to an externally applied electric field. *Engineering Structures, 42*, 201–213.

Liu, Q. F., Xia, J., Easterbrook, D., Yang, J., & Li, L. Y. (2014). Three-phase modeling of electrochemical chloride removal from corroded steel-reinforced concrete. *Construction and Building Materials, 70*, 410–427.

Liu, Q. F., Yang, J., Xia, J., Easterbrook, D., Li, L. Y., & Lu, X. Y. (2015). A numerical study on chloride migration in cracked concrete using multi-component ionic transport models. *Computational Materials Science, 99*, 396–416.

Liu, Y., & Shi, X. (2012). Ionic transport in cementitious materials under an externally applied electric field: Finite element modeling. *Construction and Building Materials, 27*, 450–460.

Narsillo, G. A., Li, R., Pivonka, P., & Smith, D. W. (2007). Comparative study of methods used to estimate ionic diffusion coefficients using migration tests. *Cement and Concrete Research, 37*, 1152–1163.

NT Build 443. (1995). *Concrete, hardened: Accelerated chloride penetration, Nordtest method*. Helsingfors, Finland.

NT-Build 492. (1999). *Nordtest method: Concrete, mortar and cement-based repair materials: Chloride migration coefficient from non-steady-state migration experiments*.

Samson, E., & Marchand, J. (2007). Modeling the transport of ions in unsaturated cement-based materials. *Computers & Structures, 85*, 1740–1756.

Šavija, B., Luković, M., & Schlangen, E. (2014). Lattice modeling of rapid chloride migration in concrete. *Cement and Concrete Research, 6*(1–62), 49–63.

Sun, G., Zhang, Y., Sun, W., Liu, Z., & Wang, C. (2011). Multi-scale prediction of the effective chloride diffusion coefficient of concrete. *Construction and Building Materials, 25*, 3820–3831.

Tang, L., & Nilsson, L. O. (1993a). Rapid determination of the chloride diffusivity in concrete by applying an electric field. *ACI Materials Journal, 89*(1), 49–53.

Tang, L., & Nilsson, L. O. (1993b). Chloride binding capacity and binding isotherms of OPC pastes and mortars. *Cement and Concrete Research, 23*, 247–253.

Toumi, A., Francois, R., & Alvarado, O. (2007). Experimental and numerical study of electrochemical chloride removal from brick and concrete specimens. *Cement and Concrete Research, 37*, 54–62.

Truc, O., Ollivier, J. P., & Nilsson, L. O. (2000). Numerical simulation of multi-species transport through saturated concrete during a migration test – MSDIFF code. *Cement and Concrete Research, 30*, 1581–1592.

Wang, Y., Li, L. Y., & Page, C. L. (2001). A two-dimensional model of electrochemical chloride removal from concrete. *Computational Materials Science, 20*, 196–212.

Whiting, D. (1981). Rapid measurement of the chloride permeability of concrete. *Public Roads, 45*(3), 101–112.

Xi, Y., & Bazant, Z. P. (1999). Modeling chloride penetration in saturated concrete. *Journal of Materials in Civil Engineering, 11*(1), 58–65.

Xia, J., & Li, L. Y. (2013). Numerical simulation of ionic transport in cement paste under the action of externally applied electric field. *Construction and Building Materials, 39*, 51–59.

Xiao, J., Ying, J., & Shen, L. (2012). FEM simulation of chloride diffusion in modeled recycled aggregate concrete. *Construction and Building Materials, 29*, 12–23.

Xu, K., Daian, J. F., & Quenard, D. (1997). Multiscale structures to describe porous media part II: Transport properties and application to test materials. *Transport Porous Med, 26*(3), 319–338.

Yang, C. C., & Weng, S. H. (2013). A three-phase model for predicting the effective chloride migration coefficient of ITZ in cement-based materials. *Magazine of Concrete Research, 65*(3), 193–201.

Ying, J. W., Xiao, J. Z., Shen, L. M., & Bradford, M. A. (2013). Five-phase composite sphere model for chloride diffusivity prediction of recycled aggregate concrete. *Magazine of Concrete Research, 65*(9), 573–588.

Zeng, Y. W. (2007). Modeling of chloride diffusion in hetero-structured concretes by finite element method. *Cement and Concrete Composites, 29*, 559–565.

Zheng, J. J., Wong, H. S., & Buenfeld, N. R. (2009). Assessing the influence of ITZ on the steady-state chloride diffusivity of concrete using a numerical model. *Cement and Concrete Research, 39*, 805–813.

Zheng, J. J., Zhou, X. Z., Wu, Y. W., & Jin, X. Y. (2012). A numerical method for the chloride diffusivity in concrete with aggregate shape effect. *Construction and Building Materials, 31*, 151–156.